Grain Boundary Penetration of a Ni-Rich Melt in Tungsten Polycrystals

V. Glebovsky[1], B. Straumal[1,2], V. Semenov[1], V. Sursaeva[1] and W. Gust[2]

[1]*Institute of Solid State Physics, Russian Academy of Sciences, Chernogolovka, Moscow District, 142432 Russia*
[2]*Max-Planck-Institut für Metallforschung and Institut für Metallkunde, Seestr. 75, D-70174 Stuttgart, Germany*

SUMMARY

The penetration of Ni along the grain boundaries (GBs) in W polycrystals at different temperatures (1600, 1800 and 2000°C) above the eutectic temperature of the W-Ni system has been investigated. At 1600°C three different groups of GBs were found: (a) GBs wetted by the Ni-rich melt; (b) GBs partially wetted by the Ni-rich melt; (c) GBs not wetted by the Ni-rich melt. This means that the GB wetting phase transition in the W-Ni system can be observed. Measurements with the aid of *selected area channelling* show that only GBs with the highest misorientation angles are wetted at 1600°C. It means that the GB wetting phase transition temperatures for the GBs with different energies lie in a wide temperature interval.

INTRODUCTION

The penetration and distribution of a liquid phase in the grain boundaries (GBs) play a very important role in liquid phase sintering of refractory metals. Complete wetting of the solid by the liquid is believed necessary for full densification during liquid phase sintering of materials containing a high volume fraction of the solid phase. The parameters of liquid phase sintering (for example, the spacing between solid particles) depend critically on the wetting angles θ at the contacts between liquid phase and particles /1,2/. Liquid bridges between particles with different θ may assume different forms /2/, and the spacing dependencies of the force between such particles are also very different for different θ /3-5/. For low wetting angles, the force F between the particles is attractive and during the sintering it presses the particles together /1/. For large values of θ, the force F is repulsive at little spacings and is attractive only at large spacings /1/. In this case, during the sintering an equilibrium spacing exists and at lower spacings the particles repel each other. This difference between the forces for large θ and low θ controls the process of particle rearrangement. The formation of necks with low energy GBs after particle coalescence can be seen particularly well in systems like Fe-Cu /6,7/ and Ag-Cu /8/. It was shown /9/ that in W-Ni alloys, during the initial stages of sintering, the original polycrystalline W powder dissolved into single crystals due to the penetration of liquid Ni along the solid GBs. However, after long sintering periods /10,11/, microstructural studies clearly indicate that some of the W single crystals move about within the liquid and subsequently contact and coalesce into a single particle. This indicates that in a certain temperature interval above the eutectic temperature T_e in the W-Ni system the low energy GBs are not wetted and the high energy GBs are wetted by the liquid phase.

If the GB energy σ_{GB} is higher than $2\sigma_{SL}$ (σ_{SL} is the energy of the liquid-solid phase boundary per unit area), the GB is wetted and $\theta = 0$ (θ is the contact angle at the site of the GB intersection with the solid-melt interface, see Fig. 1). If the σ_{GB} and σ_{SL} change differently with temperature (Fig. 1c), the so-called GB wetting phase transition at T_w can proceed /12,13/. Below T_w, $2\sigma_{SL} > \sigma_{GB}$ and $\theta > 0$, the GB is not wetted;

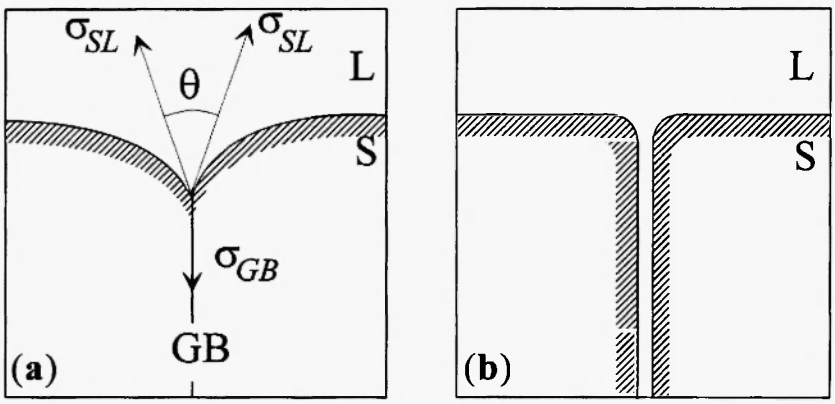

Fig. 1: Bicrystal in contact with the liquid phase (L). (a) Incomplete wetting of the GB by the melt, θ>0. (b) Complete wetting, θ=0.

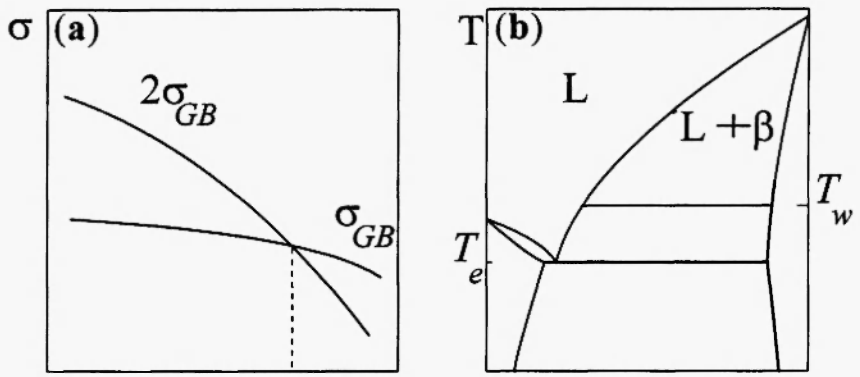

Fig. 2: (a) Schematic diagram of the temperature dependencies of the energies of the grain boundaries (σ_{GB}) and the solid liquid phase boundaries (σ_{SL}) near the GB wetting phase transition temperature T_w. (b) An idealized eutectic phase diagram for the component B with high melting temperature T_m and the component A with low T_m. The line of possible wetting GB phase transition at temperature T_w is also shown.

above T_w, $2\sigma_{SL} < \sigma_{GB}$, $\theta = 0$, and the GB is wetted (Fig. 2a). The conode in the (L+β) two-phase area (Fig. 2b) schematically shows such a GB wetting phase transition. GB wetting phase transitions have been observed in the following binary and quasi-binary systems: Zn-Sn /14,15/, Al-Sn /17,19/, Al-Pb /17/, Ag-Pb /20/, (Fe-Si)-Sn /21/, (Fe-Si)-Zn /21,22/, Cu-Bi /23/ and Cu-In /24/. Different GBs with different energies also have different wetting temperatures /24/. If $\sigma_{GB1} > \sigma_{GB2}$, then $T_{w1} < T_{w2}$. For example, in the Cu-In system the wetting phase transition at the tilt GB 77°<110> in Cu occurs at T_{w1} = 930°C and at GB 141°<110> at T_{w2} = 960°C ($\sigma_{GB1} / \sigma_{GB2} = 1.4$) /24/. In our work we investigated whether it was possible to observe the GB wetting phase transition in the W-Ni system and the difference between wetting temperatures for different GBs in W polycrystals. The other aim of this study was to make the first steps in investigating the Ni-rich melt penetration along the GBs in W at different temperatures and wetting conditions.

EXPERIMENTAL

For our experiments, tablets of pure W compact (diameter 10 mm, height 5 mm) produced by Metallwerk Plansee GmbH were used. Prior to the other experiments, these samples were recrystallized at

2000°C for 2 h in a vacuum of 10^{-8} Pa. After recrystallization, annealing the microstructure of the W specimens was investigated with the aid of scanning electron microscopy (**SEM**), optical microscopy and the selected area channelling (SAC) technique. Then a layer of Ni (about 1 mm thick) was applied on the surface of the W tablets. For this purpose the axial electron beam gun was used. The scheme of making coverage is shown in Fig. 3. The tablets have to be heated up to about 1000°C by an electron beam, and then the drop of Ni has to be made to provide good surface wetting. Usually this procedure takes about 30-40 s. Then the tablets were annealed at different temperatures (1600, 1800, 2000°C; 1 h) above the eutectic temperature of the W-Ni system (T_e = 1495°C) in a vacuum of 10^{-8} Pa. The cooling time was about 5 min. After the annealing the specimens were cut by electrospark machining and the cross-section perpendicular to the Ni-covered surface was investigated with the aid of optical microscopy and the SAC technique. With the aid of metallography, the area of Ni GB penetration in the W polycrystal was investigated and the GBs wetted, partially wetted or not wetted by Ni-rich melt were found.

The SAC technique was used in order to determine the mutual misorientation of grains which form GBs wetted, partially wetted or not wetted by the Ni-rich melt. In the usual X-ray techniques, the data come from a large number of grains due to the large diameter of the X-ray beam. In this case the analysis is tedious, time-consuming and indirect because the actual single grain cannot be identified. Transmission electron microscopy (**TEM**) is the only technique which combines spatial diffraction information with fine microstructural details. However, there are known limitations for the application of TEM (small electron transparent region of the foil and the difficulty in relating the view area to the whole specimen). Techniques which occupy a position in between X-ray analysis and TEM are based on SEM. For example, in the SAC technique all grains can be seen, and misorientations assigned in the actual image /25/. This means that many grains can be analyzed, and the overall picture of the misorientation distribution can quickly be obtained. The orientations of the grains were measured "by hand" from a channelling pattern. A grain orientation can be obtained from a screen using only a ruler and standard map. This method was adopted as a simple computer program for routine orientation measurements. It requires the operator to identify poles in the channelling pattern. Then the screen coordinates of three points on each of two pairs of lines and of one pole are entered in the computer program. These data are compared to a look-up table of rotations and interplanar spacings (band widths) in order to index these lines and thus solve the pattern. The orientation of a grain with respect to the specimen frame may be equally described both by rotation angles

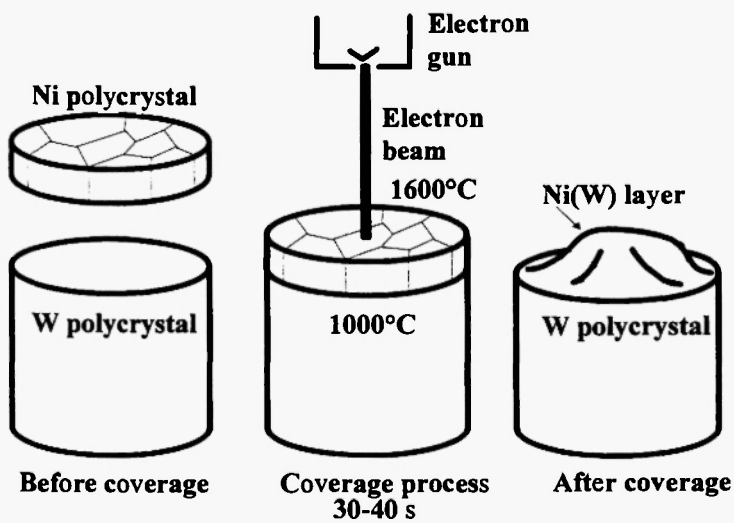

Fig. 3: Method of applying a Ni layer on the surface of a W tablet.

and rotation axes or by proper orthogonal matrices. There are 24 geometrically different, crystallographically equivalent rotations for cubic systems. Each of these rotations describes completely the orientational position of a grain with respect to the specimen frame. The direction cosines for the zone axis and for axes perpendicular to channelling planes have been determined by a primary processing of the patterns. Those with respect to grain frame were obtained via an indexing procedure. In our work, the channelling patterns and image were analyzed together. In this case the orientations can be ascribed to individual grains and related to both microscopic and macroscopic features of the specimen.

RESULTS

The investigations with the aid of optical metallography and SEM show that the microstructure of W polycrystals after recrystallization annealing (2000°C, 2 h) contains practically equiaxed grains with a size of about 30 mm (Fig. 4). But some grains in this microstructure build colonies consisting of about 20-30 grains with low-angle boundaries. Between these colonies there are the "belts" of grains with high misorientations (large central part in Fig. 4).

In Fig. 5 the microstructure of the W polycrystal is shown after penetration of the Ni-rich melt from the surface at 1600°C. This temperature lies about 100°C above the eutectic temperature of the W-Ni system. The Ni-rich phase penetrated along the GBs to a depth of about 50 μm into the W polycrystal. It can be clearly seen that in the penetration layer there are three types of GBs:

- GBs wetted with a Ni-rich melt at the annealing temperature. The Ni-rich phase formed a uniform flat thick layer on these GBs;
- GBs partially wetted with a Ni-rich melt at the annealing temperature. The Ni-rich phase formed droplets on these GBs;
- GBs not wetted with a Ni-rich melt at the annealing temperature. There are no visible macroscopic layers or particles of the Ni-rich phase on these GBs.

The misorientation parameters of 21 GBs from all three groups of GBs in the Ni-penetration layer were measured with the aid of SAC (Fig. 6). No preferential orientations (texture) were found for the grains investi-

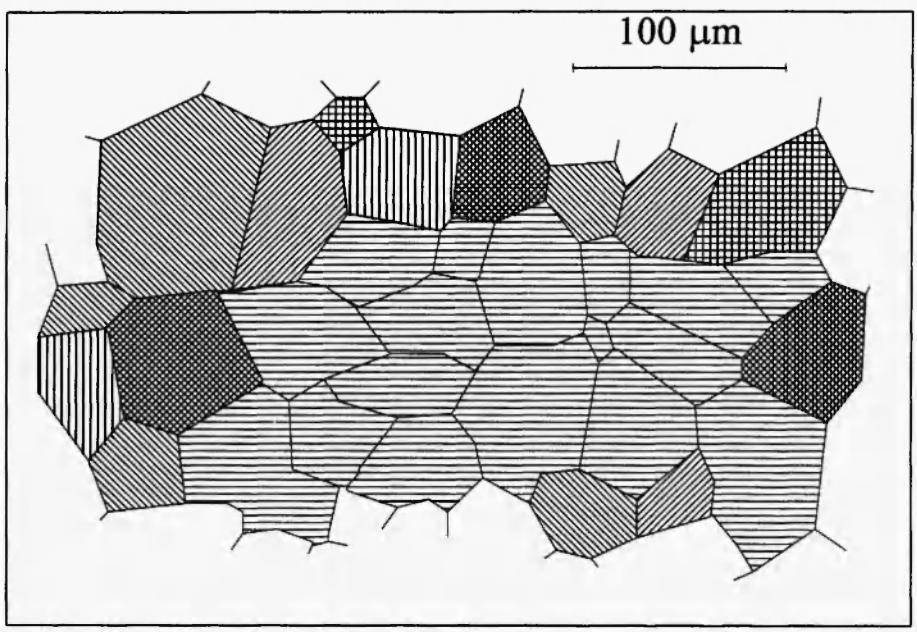

Fig. 4: The microstructure of a W polycrystal after recrystallization anneal at 2000°C for 2 h. Different shadings show different orientations of grains, measured with the aid of the selected area channelling technique.

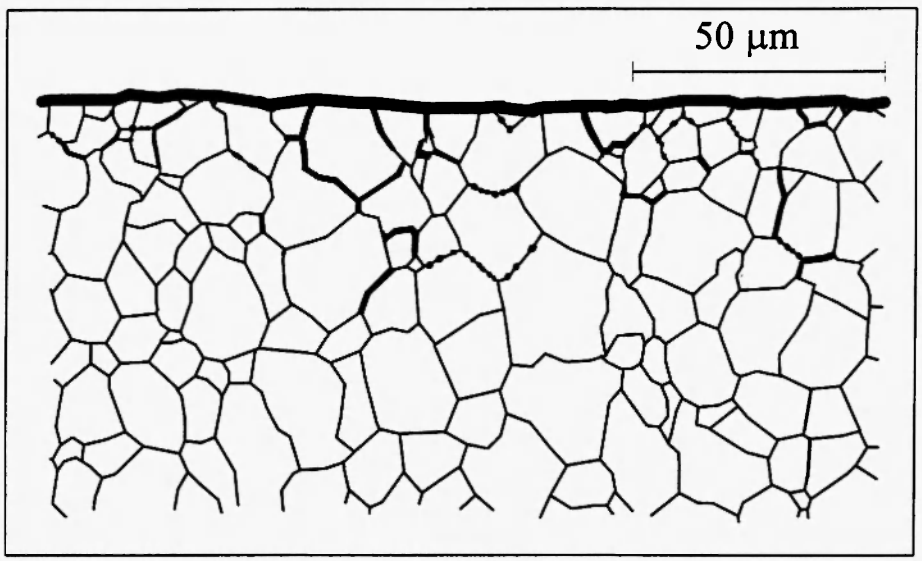

Fig. 5: The microstructure of the W polycrystal after penetration of the Ni-rich melt from the surface (top side of the figure) during annealing at 1600°C for 1 h.

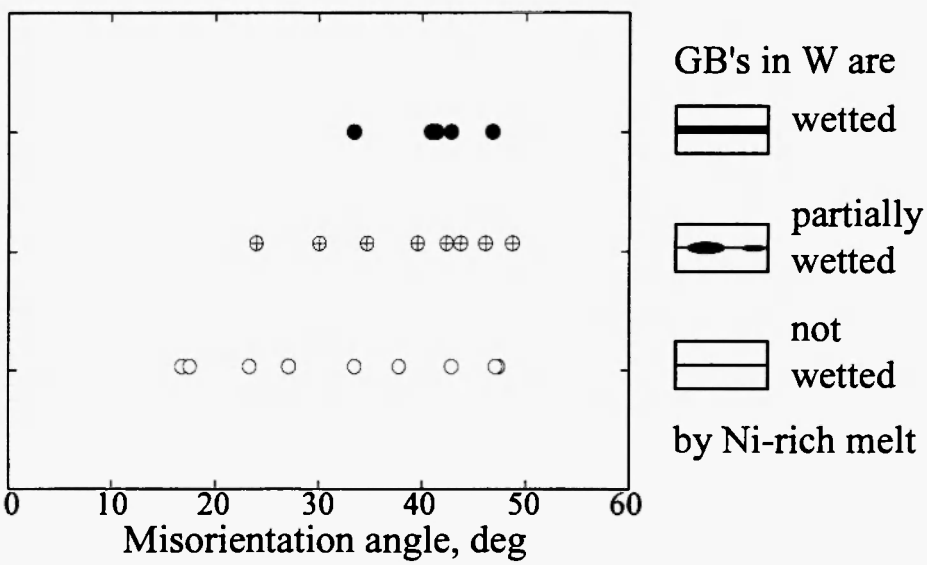

Fig. 6: The misorientations of three different groups of GBs within the Ni penetration layer of W polycrystals after anneal at 1600°C for 1 h. The misorientations were defined by the selected area channelling SEM technique.

gated. The misorientation angles q for GBs not wetted by the Ni-rich melt lie in the angular interval from 17° to 49°. The partially wetted GBs (with droplets of the Ni-rich phase) have misorientation angles from 24° top 50°. The wetted GBs (with a flat thick layer of the Ni-rich phase) have misorientation angles from 33° to 47°.

At investigated higher temperatures (1800 and 2000°C), Ni also penetrates along the GBs into the W polycrystal. But in these cases the penetration is more uniform: in the penetration layer there are no partially wetted GBs with droplets of the Ni-rich phase.

DISCUSSION

The comparison between the microstructures of W polycrystals after Ni penetration from the surface along the GBs at different temperatures shows the following:

- at 1600°C there are three different groups of GBs within the Ni penetration layer, corresponding to wetted, partially wetted and not wetted by the Ni-rich melt;
- at investigated higher temperatures there are only wetted GBs within the Ni penetration layer.

Therefore, it can be concluded that slightly above the eutectic temperature of the W-Ni system the wetting phase transition proceeds on the W grain boundaries. Moreover, the wetting phase transition proceeds on the different grain boundaries at different temperatures. The temperature of 1600°C lies in the temperature interval where different GBs in W become wetted. This conclusion is based on the observation that at 1600°C some GBs are wetted, while other GBs are partially wetted or not wetted. Therefore, the temperature interval of the GB wetting phase transition for different GBs in the W(Ni) system lies between T_e = 1495°C and 1800°C.

In Fig. 7 a sketch is shown that helps to understand the experimental misorientation distribution in the penetration layer at 1600°C (Fig. 6). In Fig. 7 the schematic misorientation dependence of the GB energy σ_{GB} is shown. At low misorientations θ, the GB energy σ_{GB} grows with θ according to the Frank formula for dislocation arrays /26/. Above θ of about 20°, the GB energy σ_{GB} grows only slightly. At high misorientations θ there are also cusps on the $\sigma_{GB}(\theta)$ dependence near the so-called coincidence misorientations. The $\sigma_{GB}(\theta)$ dependence was not experimentally measured for GBs in W, but such data exist for other cubic metals like Al /27/ and Cu /28/. In the same figure, the energy $2\sigma L$ for two solid-liquid phase boundaries of the GB wetting layer is shown. In the first approximation, $2\sigma_{SL}$ does not depend on σ. The GBs with energy $\sigma_{GB} < 2\sigma_{SL}$ are not wetted or are only partially wetted. The GBs with energy $\sigma_{GB} > 2\sigma_{SL}$ are wetted.

This sketch clearly shows that the wetted GBs must have higher misorientation angles and a narrower misorientation spectrum than the GBs that are partially

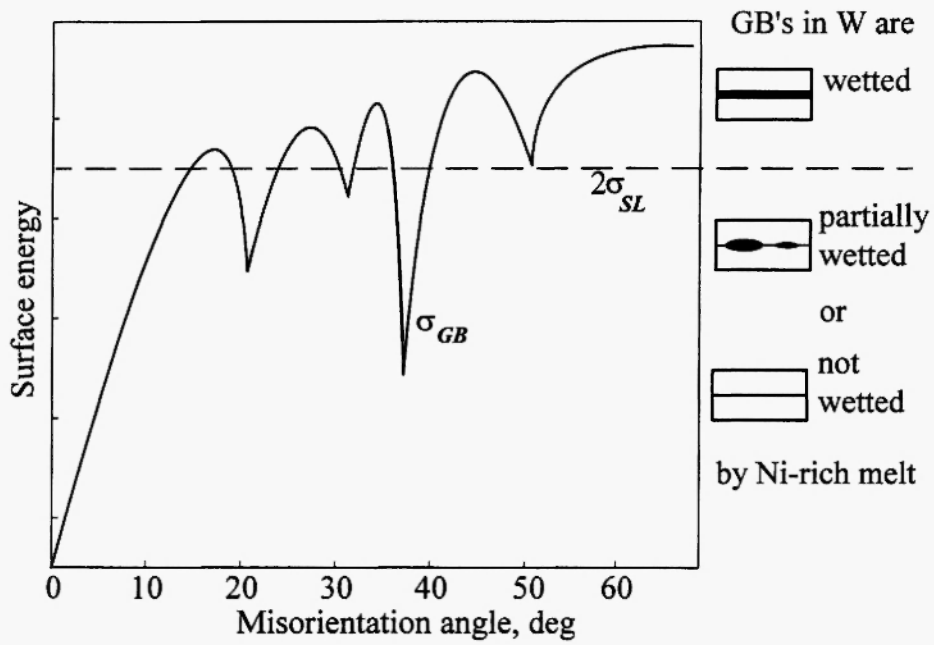

Fig. 7: Sketch showing the misorientation dependence of the GB energy $\sigma_{GB}(\theta)$ and the line for the energy $2\sigma_{SL}$ of two solid-liquid phase boundaries of the GB wetting layer.

wetted or not wetted. On the other hand, the GBs that are partially wetted or not wetted can also have a large misorientation angle if this angle lies near the custs on the $\sigma_{GB}(\theta)$ dependence, because near these cusps $\sigma_{GB} < 2\sigma_{SL}$.

ACKNOWLEDGEMENTS

The authors would like to thank Prof. L.S. Shvindlerman and Dr. E. Rabkin for many constructive ideas. We are also grateful to Prof. Chr. Herzig for providing the W samples and for helpful discussions. This work was partly supported by the International Scientific Foundation under contract RER000.

REFERENCES

1. G. Petzow and W.J. Huppmann, *Z. Metallk.*, 67, 333-342 (1976).
2. W.J. Huppmann and H. Rieder, *Acta Metall.*, b23, 965-971 (1975).
3. R.B. Heady and J.W. Cahn, *Met. Trans.*, b1, 185-191 (1970).
4. J.W. Cahn and R.H. Ready, *J. Am. Ceram. Soc.*, **53**, 406-412- (1970).
5. Yu. V. Naidich, I.A. Lavrinenko and V.N. Eremenko, *J. Powder Met.*, 1, 41-48 (1965).
6. S. Takayo, W.A. Kaysser and G. Petzow, *Acta Metall.*, **32**, 115-121 (1984).
7. W.A. Kaysser, S. Takayo and G. Petzow, *Acta Metall.*, **32**, 107-113 (1984).
8. W.A. Kaysser, S. Takayo and G. Petzow, *Z. Metallk.*, **73**, 579-586 (1982).
9. W.J. Huppmann and H. Riegger, *Int. J. Powder Met. Technol.*, b13, 243-249 (1977).
10. D.N. Yoon and W.J. Huppmann, *Acta Metall.*, **27**, 693-699 (1979).
11. D.N. Yoon and W.J. Huppmann, *Acta Metall.*, **27**, 973-979 (1979).
12. S. Dietrich, in: *Phase Transitions and Critical Phenomena*, Vol. 12, C. Domb and J. Lebowitz (eds.), Academic Press, London, 1988; pp. 1-220.
13. O.I. Noskovich, E.I. Rabkin, V.N. Semenov, B.B. Straumal and L.S. Shvindlerman, *Acta Metall.*, **39**, 3091-3096 (1991).
14. A. Passerone, N. Eustatopoulos and P. Desre, *J. Less-Common Met.*, **52**, 37-44 (1977).
15. A. Passerone and R. Sangiorgi, *Acta Metall.*, **33**, 771-777 (1985).
16. B.B. Straumal, O.I. Noskovich, V.N. Semenov, L.S. Shvindlerman, W. Gust and B. Predel, *Acta Metall. Mater.*, **40**, 795-801 (1992).
17. K.K. Ikeuye and C.S. Smith, *Trans. Am. Inst. Min. Engrs.*, **185**, 762-770 (1949).
18. N. Eustatopoulos, L. Coudurier, J.C. Joud and P. Desre, *J. Cryst. Growth*, **33**, 105-111 (1976).
19. J.H. Rogerson and J.C. Borland, *Trans. Am. Inst. Min. Engrs.*, **227**, 2-8 (1963).
20. A. Passerone, R. Sangiorgi and N. Eustatopoulos, *Scripta Metall.*, 16, 547-552 (1982).
21. E.I. Rabkin, V.N. Semenov, L.S. Shvindlerman and B.B. Straumal, *Acta Metall. Mater.*, **39**, 627-639 (1991).
22. L.S. Shvindlerman, W. Lojkowski, E.I. Rabkin and B.B. Straumal, *C. Phys.*, Coll. C1, *51*, 629-635 (1990).
23. H.J. Vogel and L. Ratke, *Acta Metall. Mater.*, **39**, 641-648 (1991).
24. B. Straumal, T. Muschik, W. Gust and B. Predel, *Acta Metall. Mater.*, **40**, 939-945 (1992).
25. V. Randle, *Microtexture Determination and its Applications*, The Institute of Metals, London, 1992; pp. 134-178.
26. W. Bollmann, *Crystal Defects and Crystalline Interfaces*, Springer Verlag, Berlin, 1970; pp. 302-352.
27. G.C. Hasson and C. Goux, *Scripta Metall.*, **5**, 889-895 (1971).
28. H. Miura, M. Kato and T. Mori, *C. Physique*, **51-C**, 263-269 (1990).